IJE TRANSACTIONS B: Applications Vol. 34, No. 05, (May 2021) 1132-1144

International Journal of Engineering

Journal Homepage: www.ije.ir

Multi-stage Performance Upgrade of Steel Moment Frames by Post-tension Connections

A. M. Heydari T., M. Gerami*

Department of Civil Engineering, Semnan University, Semnan, Iran

P A P E R I N F O

Paper history:
Received 01 February 2021
Received in revised form 29March 2021
Accepted 04 April 2021

Keywords:
Posttensioned Energy Dissipating Connection
Performance Upgrading Factor
Performance Efficiency Factor
Time History Analysis

A B S T R A C T

Numerous studies have been conducted on self-centering seismic lateral force resisting systems, the consequences of which have resulted in removing many ambiguities regarding the use of such systems in retrofitting the existing frames. The present study evaluated the new approach of improvement of multi-stage performance using such systems. Due to the significant costs of running the whole retrofit project in one stage, as well as some issues such as the impossibility of stopping the use of all floors in some of the existing buildings, multi-stage improvement can be considered as a good suggestion. In this regard, a part of the floors are retrofitted in the first stage and the next stage of improvement are then implemented by spending less budget and time. Accordingly, the execution of the first stage leads to an enhancement in the frame performance to an appropriate extent. In addition, the measuremets taken in the stage are a part of final retrofit project. In the present study, PUF and PEF coefficients were introduced and utilized to select the most appropriate pattern for applying post-tensioned connections in different floors. After analyzing frames, a model was proposed for the multi-stage improvement of each frame by selecting the appropriate pattern using post-tensioned connections in the floors. In the first stage of the suggested plan, for 3-, 6-, and 10-story frames the performance improvements were 15.3, 11.4, and 8.5%, respectively.

***doi**: 10.5829/ije.2021.34.05b.07*

NOMENCLATURE

PUF		$A_{ED}(cm^2)$	The ED element area
PEF	Performance Efficiency Factor	L_{ED}(cm)	The ED element unbonded length
RPI	Performance Upgrading Factor	$F_{int,PT}$(%FU)	The PT initial prestress force
PT	Post-Tensioned Element	M_w	The moment magnitude scale
ED	Energy Dissipator	t_d(s)	The time duration of earthquake
PTED	Posttensioned Energy Dissipating Connection	RJB(km)	Joyner-Boore distance
SLV	The slaving constrains	PGA(g)	Peak ground acceleration
K_{PT}(Tonf/Cm)	The PT element stiffness	PGV(cm/s)	Peak ground velocity

1. INTRODUCTION

The use of post-tensioning method is considered as one of the solutions to reduce or eliminate residual deformations in the main members of the structure. Applying such systems was examined by researchers in concrete structures [1-3] and then by those specilized in steel ones [4-6], all of whom reported a decrease in permanent drifs by utlizing the system. Additionally, some studies focued on the effect of the changes in each of the effective parameters in such connections [7, 8], and some others highlihted the effect of such systems on retrofitting weak connections, as well as seismic sequencing [9,10].

Post-tension connection with energy dissipating elements (PTED) is one of the modes of reversible systems in steel bending frames that has been introduced and evaluated by researchers [11]. PTED connection includes high strength steel (PT) rebars parallel to the beam axis, and the energy dissipating (ED) bars at the top and bottom of the beam on both the

*Corresponding Author Institutional Email: mgerami@semnan.ac.ir (M. Gerami)

Please cite this article as: A. M. Heydari T., M. Gerami, Multi-stage Performance Upgrade of Steel Moment Frames by Post-tension Connections, International Journal of Engineering, Transactions B: Applications Vol. 34, No. 05, (2021) 1132-1144

left and right sides of the web (Figure 1). The PT bars provide a restoring force which the frame to its initial state after an earthquake. The ED bars embedded in steel cylinders, can be yield under the axial force, leading to energy dissipation. Energy dissipation in the PTED structure is limited to the ED element only and no significant nonlinear deformation occurs in the beam and column elements [12].

Generally, a significant development was made in the field of self-centering reversible seismic systems due to their ability to reduce post-earthquake structural repair costs in recent years [13]. In this regard, different modes of the self-centering moment frame systems were suggested by some researchers [14-16]. In all of the proposed cases, the damage to the main elements of the structure reduced through the gap opening mechanism

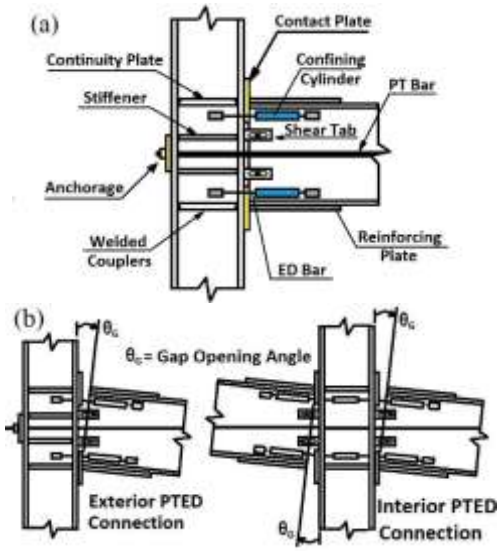

Figure 1. The schematic representation of the posttensioned connection with the energy dissipating elements (a) and gap opening on external and intermediate connection (b) [11]

between the beam and column. In general, after experiencing a major earthquake, it is only necessary to replace the energy dissipating elements in self-centering systems [17].

The novelty of this study is to proposal that in improving a steel moment frame using post-tension connections, instead of all the floors being improved in one stage, only a few floors should be reinforced in the first stage with post-tension connections. Then, in the next stages, the final improvement plan will be implemented, which can lead to economic savings. In other words, after completing some stages of the improvement operation, some floors will have conventional welded joints and some floors will have self-centered connections. In this research, PTED connection was selected and modeled for evaluations among the types of self-centering steel moment systems.

In order to retrofit the frame with welded connections the load on the frame is removed by installing the jacks under the beam element in the first step. In the next step, the top, seat, and shear plates of the beam-column connection are removed. Then the contact plates are welded to the column flange and new shear plates with horizontal slot holes are added to the beam-column connection. Then the columns are drilled to pass the PT elements and the contact elements are welded to the outer flange of the perimeter columns to resist the punching stress caused by the post-tensioning force. Finally, PT elements are post-tensioned and the jacks are removed (Figure 2).

2. VALIDATION

Various approaches have been proposed to model the PT connection-based moment frame structures. These solutions include finite element modeling [18- 20] and modeling with introducing post-tension members by

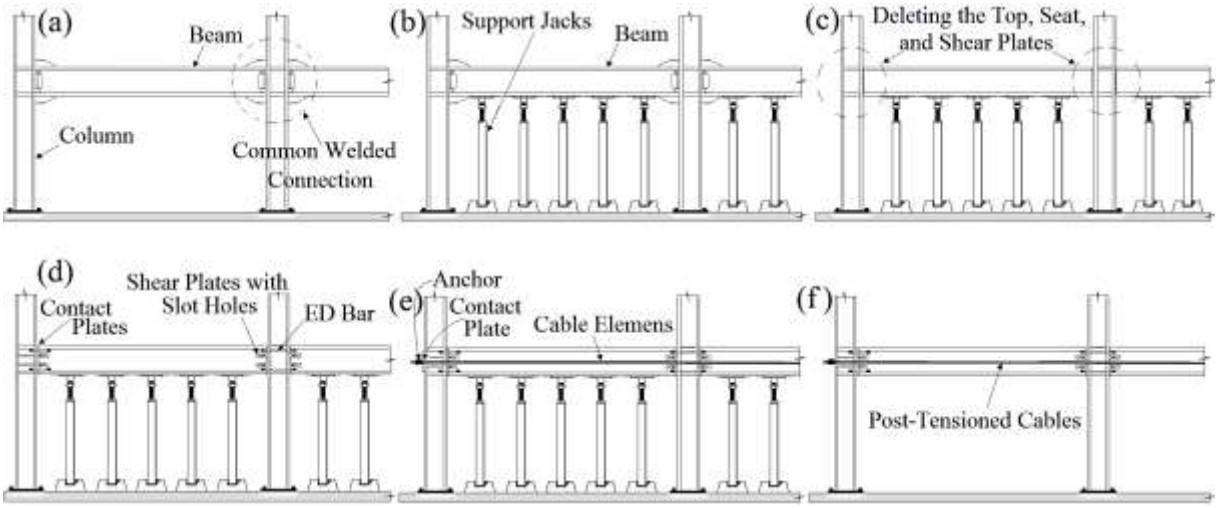

Figure 2. Erection details of retrofitting moment frame with welded connections using post-tensioned elements

the spring element [21]. Prolonged analysis and lack of direct external reflection of the behavior of the connection members leads to the abandonment of the use of finite element and spring modeling, respectively. Finally, separate modeling of the connection elements is considered in Perform-3d [22] software to increase the applicability, as well as reducing the analysis time.

The experimental study of Christopoulos et al. [11] is intended to assess the accuracy of the modeling procedure (Figure 3). A PTED beam-column connection under cyclic loading is evaluated based on the SAC loading protocol. Then, as shown in Figure 4, the elements of beam, column, rigid, connection, ED and PT are modeled in Perform-3d software. The displacement of all nodes is restricted to H_2 to provide two-dimensional frame performance. According to experimental research, the beam and column sections are assigned to W24 × 76 and W14 211, respectively.

Modeling the PT and ED elements is performed as steel bar. The tension-only and none-buckling nonlinear steel materials were used to introduce PT and ED, respectively. The experimental study indicates that a cross-section of 3.8 cm^2 (each cable diameter is 46 mm) and 16.9 cm^2 is provided for the cable and PT elements, respectively. The specifications of DSI high strength bars with elasticity modulus, the final stress and the yield stress are 1.9×10^6, 10500 and 8500 kg/cm^2, respectively, which assigned to the cables and the DSI threaded bars specifications with elasticity modulus, the final stress and the yield stress are 2.038×10^6, 6000 and 4200 kg/cm^2, respectively, which assigned to the ED element. An initial strain equivalent to 0.0028 was applied to the cables to provide posttension until the axial force of 655 KN is created similar to the experimental work in the beam element. The contact element is nonlinear elastic gap hook bar with a low tensile stiffness to provide gap opening which is modeled with a compressive stiffness of 4.62×10^7 Kg_f/cm. The rigid element is defined from non-standard zero-dimensional sections with high axial, shear and moment resistances with high inertia to ensure its rigid performance. Finally, as shown in Figure 4, the elements of beam, column, rigid, PT, ED and contact are modeled. Some constraints between different nodes to ensure system performance are also presented in Table 1.

Then the cyclic load simulation is performed by introducing 30 cycles as gravity load, with positive coefficients for positive and negative coefficients to and fro loads, respectively, as well as applying drift constraints in each cycle to stop the analysis and subsequent cumulative application of these weight loads. In addition, the output end of each cycle is extracted separately and added to the output end of the previous cycles with a negative coefficient. Finally, the structural response under cyclic loading is illustrated in Figure 5, which is in line with the results of the experimental study.

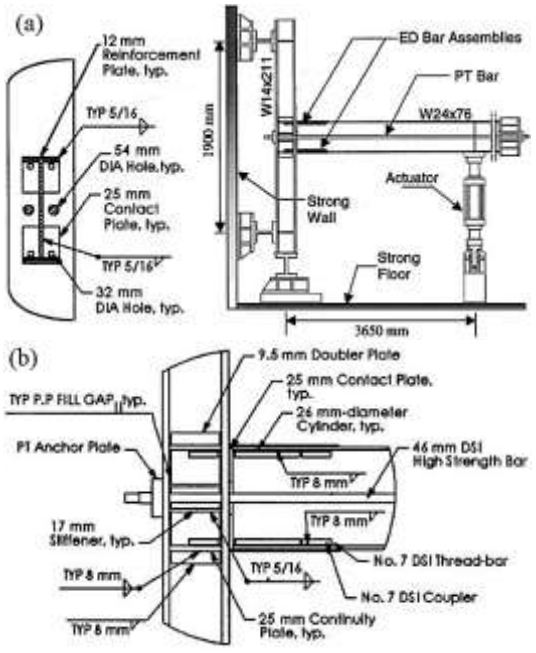

Figure 3. Overview of the experimental model of connection after stress with energy dissipating elements (a) and display of its connection details (b) [11]

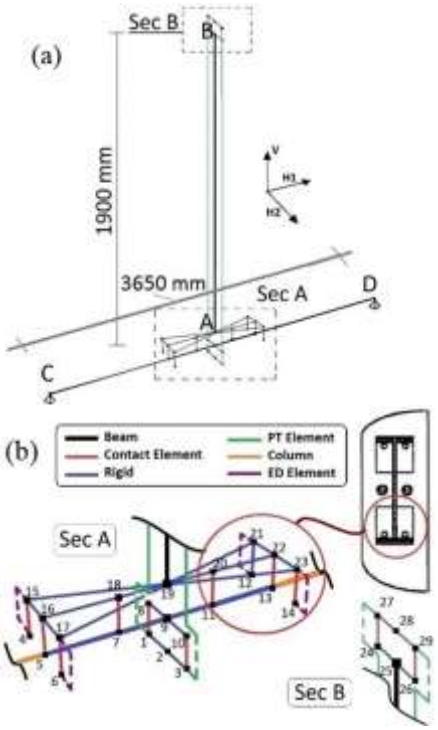

Figure 4. Overview of beam-column modeling with PTED connection (a) and details of the A and B sections (b)

TABLE 1. The constraints applied between nodes

	Node Number									
SLV	**1-3**	**4-5 6-8 10-12 13-14**	**2-9-19**	**4-5-6-8 10-12 13-14**	**15-16-17**	**15-16 17-18 20-21 21-23**	**21-22-23**	**24-25 26-27 28-29**	**5-9-13**	**24-25 26-27 28-29**
H1	✓	✓	✓			✓		✓		
V			✓	✓	✓		✓			✓
R2					✓		✓		✓	
RV	✓	✓				✓		✓		

SLV: Terms H1 and V are displacement in H1 and V direction and R2 and RV rotation around H2 and V axis respectively.

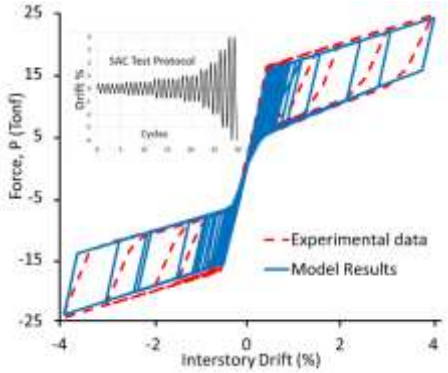

Figure 5. Experimental and numerical force interstory drift

3. MODELING

In this study, three-, six-, and ten-story structures were evaluated. The perimeter frames are in the east-west direction of the special moment frame and the north-south direction of the braced frame. Internal frames tolerate the gravity load while perimeter frames tolerate the lateral loads. The plan of all three structures is similar, as shown in Figure 6.

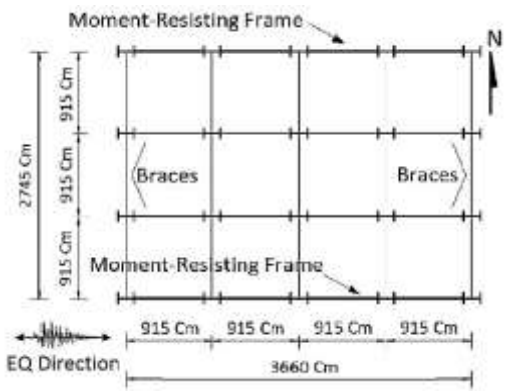

Figure 6. Plane view of structures evaluated in this study

The three-story structure used in the present study was first designed by Shen et al. [23], and then re-designed and evaluated by Apostolakis et al. [24] (Figure 7a). Then PTED connection is used to provide moment resistance of the frame by Apostolakis et al. [25]. The frame with similar specifications as the PTED connections frame designed by Apostolakis et al. [25] was modeled and the result of the push-over analysis is shown in Figure 7b. In addition, the results shown in Figure 7b confirm the validity of the modeling procedure performed in this study.

The six- and ten-story structure was designed in both cases with the welded (Figures 8a and 8b) and PTED connections across all stories based on Apostolakis et al. [25] proposed procedure through plans, loading, codes and the specifications similar to the mentioned three-story structure. The modeling parameters of PTED

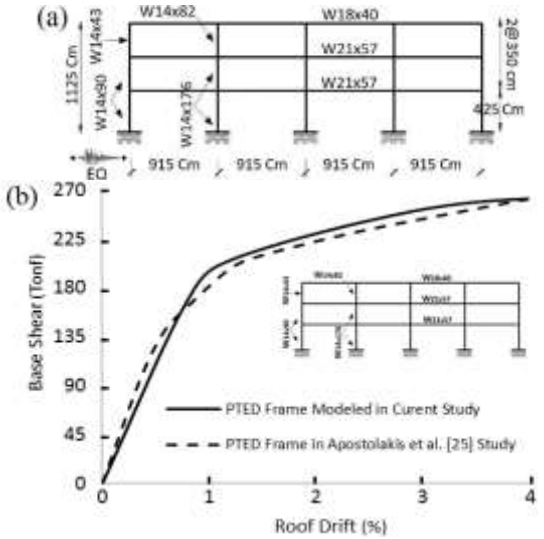

Figure 7. Elevation view (a) and structural pushover curves (b) of three-story frame in Apostolakis et al. [25] and current research

connections in all three-, six- and ten-story structures are shown in Table 2.

Seven states for the three-story frame, ten states for the six-story frame and fourteen states for the ten-story frame were evaluated based on the engineering judgment to evaluate the different states of the post-tensioned distribution in the floors. The different statuses and the nomenclature of the frames are shown in Table 3. For example, the frame with the abbreviation s-1 is a six-story frame which the PTED connections is used in the first and second floors.

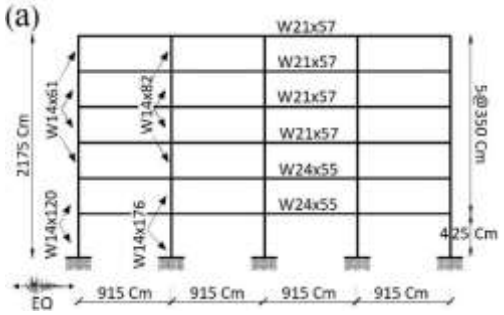

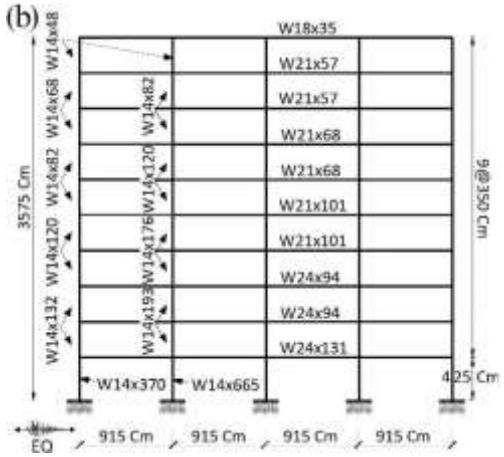

Figure 8. Elevation view of six-story (a) and ten-story (b) frames that are examined in this research

4. ANALYSIS

The time history analysis was performed on eight three-story frames, eleven six-story frames and fifteen ten-story frames (presented in Table 3). In the time history

TABLE 2. The PTED parameters of 3-, 6- and 10-story frames

	Story	Three- and six-story				Story	Ten story			
		K_{PT}(tonf/ Cm)	A_{ED} (Cm^2)	L_{ED} (Cm)	$F_{init,PT}$ (%FU)		K_{PT}(tonf/ Cm)	A_{ED} (Cm^2)	L_{ED} (Cm)	$F_{init,PT}$ (%FU)
3-story	St1	6	7	58.4	0.3	St1	9	9.5	64.3	0.32
	St2	6	7	38.1	0.36	St2	9	9.5	64.3	0.32
	St3	9	5.8	58.1	0.26	St3	9	8.5	58.4	0.36
						St4	6	8.5	58.4	0.36
6-story	St1	9	8.5	58.4	0.3	St5	6	8.5	58.4	0.36
	St2	9	8.5	58.4	0.3	St6	6	7	38.1	0.3
	St3	6	7	58.4	0.36	St7	6	7	38.1	0.3
	St4	6	7	38.1	0.36	St8	9	7	38.1	0.3
	St5	9	5.8	38.1	0.26	St9	9	5.8	37	0.26
	St6	9	5.8	38.1	0.26	St10	9	5.8	37	0.26

TABLE 3. Distribution of PT connections in floors

3-story		6-story		10-story	
Frame	**PT Stories**	**Frame**	**PT Stories**	**Frame**	**PT Stories**
3st-MRF	No story	6st-MRF	No story	10st-MRF	No story
3st-PTED	All stories	6st-PTED	All stories	10st-PTED	All stories
t-1	1	s-1	1,2	Te-1	1,2
t-2	2	s-2	3,4	Te-2	1,2,5,6
t-3	3	s-3	5,6	Te-3	1,2,6,7
t-4	1,2	s-4	1,2,3	Te-4	1,2,7,8
t-5	1,3	s-5	2,3,4	Te-5	1,2,6,7,8
t-6	2,3	s-6	3,4,5	Te-6	1,2,5,6,7,8
		s-7	4,5,6	Te-7	1,2,3
		s-8	2,3,4,5	Te-8	1,2,3,5,6
		s-9	1,2,3,4	Te-9	1,2,3,6,7
				Te-10	1,2,3,7,8
				Te-11	1,2,3,6,7,8
				Te-12	1,2,3,5,6,7,8
				Te-13	1,2,3,4,5,6

analyses of this study, the record to record variability is considered by employing a set of 15 ground motion records representative of different intensities, durations and frequency contents, adopted from the FEMA P-695 [26]. The characteristics of the selected ground motion records are provided in Table 4.

Similar to Apostolakis et al. [25] study, maximum and residual drift, and maximum and RMS acceleration were considered as performance evaluation of the structural parameters. RMS parameter demonstrates root mean square floor acceleration, which is calculated based on Equation (1):

$$\mathrm{RMSAcc} = \max\left\{\sqrt{\frac{\sum_{j=1}^{N}\left[Acc_i\left(t_j\right)\right]^2}{N}}\right\} \quad \text{for} \quad i=1,\ldots,N_{story} \qquad (1)$$

where N and Acc_i (t_j) are the number of time steps within the actual duration of an earthquake (t_d in Table 4) and the absolute acceleration of the story i at the time step j, respectively. Figure 9 displays the values of the above-mentioned parameters for three-, six-, and ten-story frames with conventional welding connections (3st-MRF, 6st-MRF and 10st-MRF).

5. ASSESSING THE COMPETENCY OF EACH FRAME

The overall upgrading effect associated with retrofitting by post-tension connections was quantified by a relative performance index (RPI), which combines several single-parameter indices (SPIs), including peak interstory drift ratios, residual interstory drift ratios, peak floor accelerations, and root mean square floor accelerations [27, 28] (Equation (2)). In this regard, the mentioned parameters were evaluated for each frame and then only a single numerical parameter is assigned to the relative performance of each frame using RPI, which has led to the use of this evaluation procedure instead of other evaluation methods such as incremental dynamic analysis.

$$\begin{aligned} &\mathrm{RPI} = \alpha\times\mathrm{MDR} + \beta\times\mathrm{RDR} + \gamma\times\mathrm{RMSAR} + \delta\times\mathrm{MAR} \\ &\mathrm{MDR} = \frac{\mathrm{MaxDrift}_{\mathrm{Frame}}}{\mathrm{MaxDrift}_{\mathrm{MRF}}} \quad ; \quad \mathrm{RDR} = \frac{\mathrm{ResDrift}_{\mathrm{Frame}}}{\mathrm{ResDrift}_{\mathrm{MRF}}} \\ &\mathrm{RMSAR} = \frac{\mathrm{RMSAcc}_{\mathrm{Frame}}}{\mathrm{RMSAcc}_{\mathrm{MRF}}} \quad ; \quad \mathrm{MAR} = \frac{\mathrm{MaxAcc}_{\mathrm{Frame}}}{\mathrm{MaxAcc}_{\mathrm{MRF}}} \end{aligned} \qquad (2)$$

In Equation (2), the parameters MaxDrift, ResDrift, RMSAcc and MaxAcc are Maximum interstory drift, residual interstory drift, root mean square floor acceleration and max floor absolute acceleration, respectively, and root mean square floor acceleration values are calculated based on Equation (1). The coefficients α, β, γ and δ in Equation (2) are weighting coefficients, the sum of which is equal to one and can have values ranging from 0 to 1.

Based on Table 5, 15 various states for the values of weighting coefficients were considered in the present study to select the optimal frame with more accuracy.

In addition, each frame was first analyzed by applying 15 earthquake records (presented in Table 4). Further, the mean of 15 frame responses was extracted and their maximum was computed and used in the calculations of Equation (2). Furthermore, the weight coefficients corresponding to each scenario (Table 4) were replaced in Equations (2) and (15) values were calculated for RPI.

TABLE 4. The ground motion characteristics

Name	Earthquake event	Year	Station	M_W	t_d (s)	RJB (km)	PGA (g)	PGV (Cm/s)
EQ1	Northridge	1994	Beverly Hills-Mulhol	6.7	30	9.4	0.488	63
EQ2	Northridge	1994	Canyon Country-WLC	6.7	20	11.39	0.471	45
EQ3	Duzce, Turkey	1999	Bolu	7.1	56	12	0.805	62
EQ4	Hector Mine	1999	Hector	7.1	45	10.3	0.328	42
EQ5	Imperial Valley	1979	Delta	6.5	100	22	0.349	33
EQ6	Imperial Valley	1979	El Centro Array #11	6.5	39	12.5	0.379	42
EQ7	Kobe, Japan	1995	Nishi-Akashi	6.9	41	7	0.483	37
EQ8	Kobe, Japan	1995	Shin-Osaka	6.9	41	19.1	0.233	38
EQ9	Kocaeli, Turkey	1999	Duzce	7.5	27	13.6	0.364	59
EQ10	Kocaeli, Turkey	1999	Arcelik	7.5	30	10.5	0.21	40
EQ11	Landers	1992	Yermo Fire Station	7.3	44	23.6	0.244	52
EQ12	Landers	1992	Coolwater	7.3	28	19.7	0.417	42
EQ13	Loma prieta,USA	1989	Capitola	6.9	40	8.6	0.511	35
EQ14	Loma prieta,USA	1989	Gilroy Array #3	6.9	40	12.2	0.559	45
EQ15	Manjil, Iran	1990	Abbar	7.3	53	12.5	0.514	54

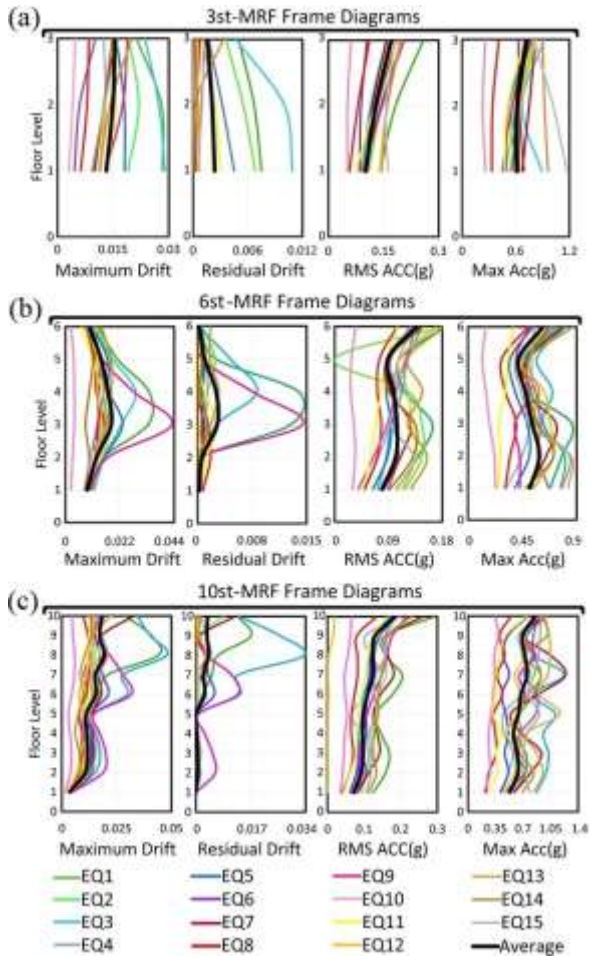

Figure 9. Schematic Diagrams of 3st-MRF (a), 6st-MRF (b) and 10st-MRF (c) frame responses (Maximum drift, Residual drift, RMS acceleration and Maximum acceleration) under earthquakes mentioned in Table 4

TABLE 5. The values considered for α, β, γ and δ

	Different scenarios for RPI															
Weight Factor	**RPI_1**	**RPI_2**	**RPI_3**	**RPI_4**	**RPI_5**	**RPI_6**	**RPI_7**	**RPI_8**	**RPI_9**	**RPI_{10}**	**RPI_{11}**	**RPI_{12}**	**RPI_{13}**	**RPI_{14}**	**RPI_{15}**
α	1	0	0	0	1/4	0	1/3	1/3	1/3	1/3	1/6	1/6	1/6	1/3	1/3
β	0	1	0	0	1/4	1/3	0	1/3	1/3	1/3	1/6	1/3	1/3	1/6	1/6
γ	0	0	1	0	1/4	1/3	1/3	0	1/3	1/6	1/3	1/6	1/3	1/6	1/3
δ	0	0	0	1	1/4	1/3	1/3	1/3	0	1/6	1/3	1/3	1/6	1/3	1/6

Finally, the RPIs were averaged and the final value of the performance index related to each frame was determined.

5. 1. Upgrade and Effectiveness of Each Frame

The inverse of RPI can be utilized to determine the degree of improving or reducing the frame performance relative to moment frame so that RPI greater than one reflects upgrading performance vice versa. Accordingly, performance upgrade factor (PUF) was introduced based on Equation (3) for the first time in this study to calculate the degree of increasing the performance of each frame in relation to the moment frame.

$$PUF = \frac{1}{RPI} - 1 \quad (3)$$

Additionally, performance efficiency factor (PEF) was provided and used based on the Equation (4) in order to examine the efficiency of utilizing PT connections in each floor. In fact, the coefficient allows to calculate the effect of using PT connection per story so that the state with the highest PEF indictaes obtaining the maximum performance improvement by using PT connections in the lowest number of floors. Accordingly, considering PEF during suggesting a retrofitting plan for an existing structure is important when requiring more cost-effective PT systems.

$$PEF = \frac{PUF}{n} \quad (4)$$

where n illustrates the number of the stories in which PT connections are applied. It is worth noting that PEF values less than zero represent the negative efficiency of utilizing PT connection in each floor.

Tables 5, 6, and 7 summarize the RPI, PUF, and PEF values of each frame. As demonstrated, the normalized PUF values are presented as NPUF parameter in the fifth column, which are considered as the ratio of the PUF related to each frame to the maximum PUF of frames with similar floors.

Based on the results in Table 6, the least RPI was observed in 3st-PTED (0.829) and t-4 frames (0.829), while the highest was related to t-2 (0.968) and t-3 frames (0.964).

The PUF and PEF values of three-story frames are represented in Figure 10. As shown, all states result in

TABLE 6. Competency assessment values for 3-story frames

Frame	PT Stories	RPI	PUF	NPUF	n	PEF
3st-PTED	All Stories	0.825	0.233	100 %	3	0.078
t-1	1	0.875	0.153	65.9 %	1	0.153
t-2	2	0.968	0.035	14.9 %	1	0.035
t-3	3	0.964	0.039	16.6 %	1	0.039
t-4	1,2	0.829	0.232	99.5 %	2	0.116
t-5	1,3	0.857	0.177	75.9 %	2	0.088
t-6	2,3	0.940	0.066	28.4 %	2	0.033

enhancing the performance of the frame compared to that of frame with conventional welded connections (PUF>1). Further, 3st-PTED (0.233) and t-4 frames (0.232) attain the maximum PUF, while t-1 (0.153) and t-4 frames (0.116) achieve the highest PEF .

In order to increase the performance of three-story frames during multi-stage, two scenarios were proposed based on the values presented in Figure 10 and Table 6. The first scenario includes upgrading the frame to t-5 one in the first stage and 3st-PTED one during the next stages. Due to the low value of PEF in t-5 and 3st-PTED frames, the scenario failed to provide the economic savings intended in the study. Therefore, the second scenario was proposed, upon which the frame is upgraded to t-1 in the first stage (65.9% of the final performance improvement), t-4 in the second stage (99.5% of the final improvement), and finally, 3st-PTED frame in the third step if an upgrade to 23.3% is considered (Figure 11).

According to the proposed improvement scenario, the response diagrams of t-1 and t-4 frames are represented in Figures 12a and 12b. Furthermore, Figure 12c demonstrates the mean response of t-1, t-4, 3st-PTED, and 3st-MRF frame diagrams for easifying comparison. As displayed, the t-1, t-4, and 3st-PTED

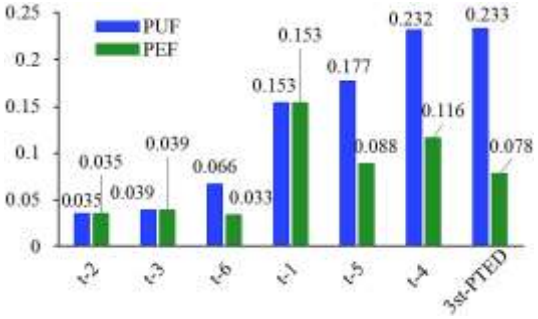

Figure 10. PUF and PEF values of 3-Story frames

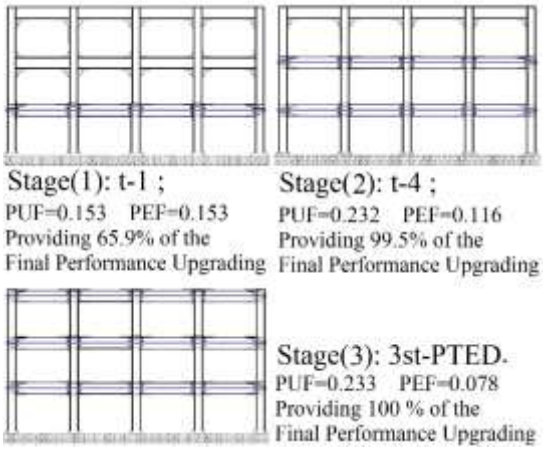

Figure 11. Proposed scenario for multi-stage retrofitting of three-story frame

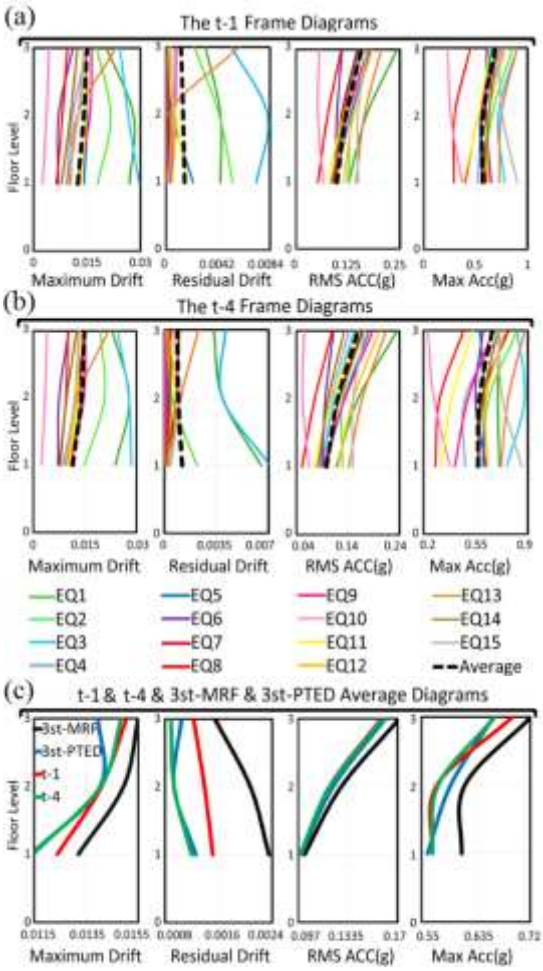

Figure 12. Schematic Diagrams of t-1 (a), t-4 (b) and average of t-1, t-4, 3st-MRF and 3st-PTED (c) frame responses under earthquakes mentioned in Table 4

frames provide a more appropriate response compared to the 3st-MRF one. The response of 3st-PTED frame at maximum dirift, and that of t-4 frame at residual dirift and maximum acceleration are better than that of other frames, while the RMSAcc response of frames t-1, t-4, and 3st-PTED are almost identical.

Considering the values of RPI, PUF, NPUF, n, and PEF of six-story frames (Table 7), the RPI coefficients of the frames s-3, s-6, and s-7 are higher than one. This issue reflects that the conversion of the frame with conventional welded connections to the intended frames in all floors results in decreasing the performance of the frame instead of enhancing the performance.

Figure 13 depicts the PUF and PEF for six-story frames, which are sorted based on the largest values. As shown, the highest PUF is obtained in s-9 (0.301) and 6st-PTED frames (0.239), while the maximum PEF is achieved in s-9 (0.075) and s-1 frames (0.057).

Based on the PUF and PEF values in Table 7 and Figure 13, two scenarios were proposed to enhance the

TABLE 7. Competency assessment values for 6-story frames

Frame	PT Stories	RPI	PUF	NPUF	n	PEF
6st-PTED	All stories	0.83	0.239	79.4 %	6	0.040
s-1	1,2	0.90	0.113	37.8 %	2	0.057
s-2	3,4	0.96	0.045	14.9 %	2	0.023
s-3	5,6	1.63	-0.334	---	2	-0.167
s-4	1,2,3	0.90	0.122	40.5 %	3	0.041
s-5	2,3,4	0.88	0.153	51 %	3	0.051
s-6	3,4,5	1.09	-0.077	---	3	-0.025
s-7	4,5,6	1.39	-0.247	---	3	-0.082
s-8	2,3,4,5	0.998	0.002	0.5 %	4	0.0004
s-9	1,2,3,4	0.802	0.301	100 %	4	0.0753

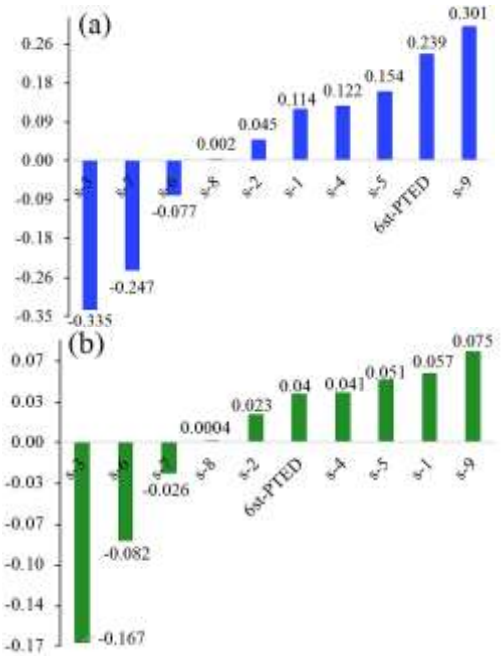

Figure 13. PUF (a) and PEF (b) values of 6-Story frames

frame performance during multi-stages (Figure 14). Regarding the first scenario, the frame was upgraded to s-1 in the first step and finally to s-9. The second scenario was suggested if an enhancement in performance by 37.8% of the final performance upgrade (performance improvement provided by s-1 frame) was insufficient for the first stage. In the second scenario, the frame was upgraded to s-5 in the first stage (leading to 51% of final performance improvement) and s-9 in the final stage. In the first scenario, an enahncement in performance was low in the first stage although it was more economical due to the larger PEF value of s-1 frame compared to that of s-5 one.

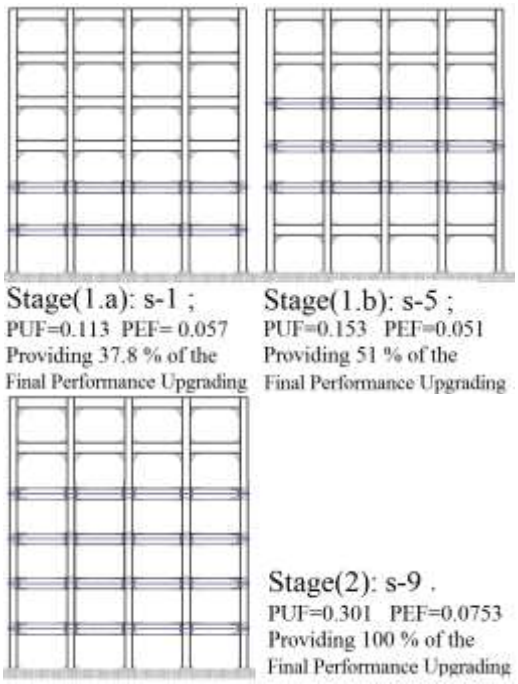

Figure 14. Proposed scenario for multi-stage retrofitting of six-story frame

Figures 15a and 15b display the response diagrams of frames s-1 and s-9. In order to compare better, Figure 15c depicts the mean response of the s-1 and s-9 frame diagrams providing the highest PEF values, as well as that of 6st-PTED and 6st-MRF frames. As demonstrated, the maximum response values of drift and residual drift in the s-1, s-9 and 6st-PTED frames reduce relative to those of the frame with welded connections in all floors, while the MaxAcc and RMSAcc diagrams of all four frames are almost identical.

In addition, ten-story frames were evaluated, the RPI, PUF, NPUF, n, and PEF of which are summarized in Table 8. Based on the results in Table 8, RPI was minimized and maximized in 10st-PTED (0.882) and Te-7 frames (0.984), respectively.

Figure 16 presents the PUF and PEF values for ten-story frames, which are sorted by largest values, which indicates the highest PUF in 10st-PTED (0.14) and Te-2 frames (0.09), as well as the maximum PEF in Te-2 (0.021) and Te-4 ones (0.016).

Considering the PUF and PEF in Table 8 and Figure 16, two scenarios were suggested for increasing the frame performance in multi-stages (Figure 17). The first scenario includeed improving the frame to Te-2 in the first stage and finally upgrading to 10st-PTED. Given that the PEF value of Te-2 frame was maximum among that of all ten-story frames, the use of the scenario was the most economical mode of improvement. The second scenario was proposed for the cases in which the start of

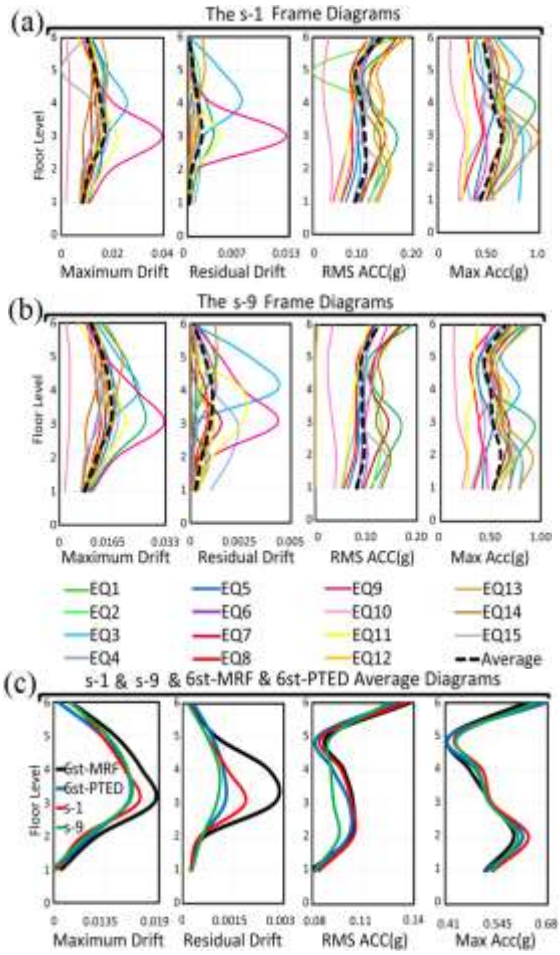

Figure 15. Schematic Diagrams of s-1 (a), s-9 (b) and average of s-1, s-9, 6st-MRF and 6st-PED (c) frame responses

TABLE 8. Competency assessment values for 10-story frames

Frame	PT Stories	RPI	PUF	NPUF	n	PEF
10st-PTED	All Stories	0.882	0.142	100 %	10	0.0142
Te-1	1,2	0.979	0.022	15.7 %	2	0.0111
Te-2	1,2,5,6	0.923	0.085	60.1 %	4	0.0213
Te-3	1,2,6,7	0.957	0.046	32.7 %	4	0.0116
Te-4	1,2,7,8	0.943	0.063	44.7 %	4	0.0159
Te-5	1,2,6,7,8	0.933	0.074	52 %	5	0.0147
Te-6	1,2,5,6,7,8	0.929	0.078	55.3 %	6	0.0131
Te-7	1,2,3	0.984	0.016	11.4 %	3	0.0054
Te-8	1,2,3,5,6	0.928	0.078	55.4 %	5	0.0157
Te-9	1,2,3,6,7	0.980	0.021	14.5 %	5	0.0041
Te-10	1,2,3,7,8	0.949	0.056	39.7 %	5	0.0112
Te-11	1,2,3,6,7,8	0.941	0.064	45.1 %	6	0.0107
Te-12	1,2,3,5,6,7,8	0.943	0.061	43.2 %	7	0.0087
Te-13	1,2,3,4,5,6	0.935	0.069	48.7 %	6	0.0115

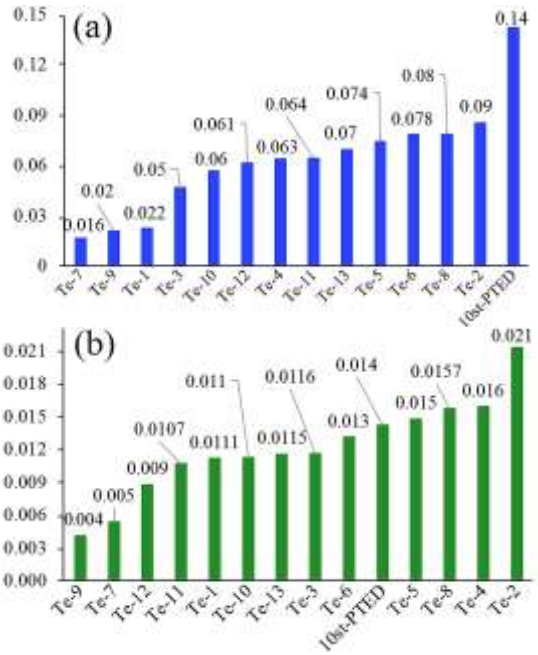

Figure 16. PUF (a) and PEF (b) values of 10-Story frames

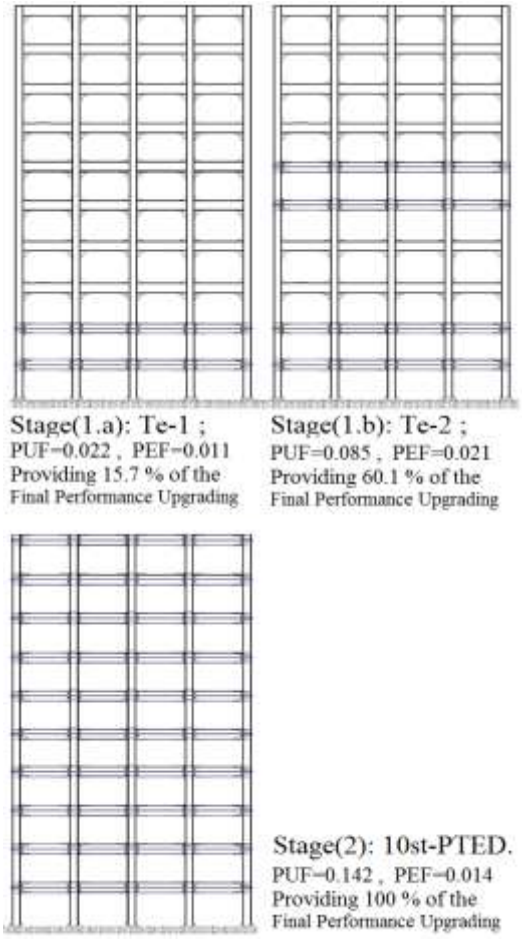

Figure 17. Proposed scenario for multi-stage retrofitting of ten-story frame

upgrade by using PT connections in four floors is impossible due to the lack of retrofit budget or similar cases. In the scenario, the frame was upgraded to the Te-1 by improving only two floors in the first stage. Then, it was respectively upgraded to Te-2 and 10st-PTED frames in the second and third stages. The scenario led to 15.7 and 60.1% of the final performance improvement in the first and second stages, respectively.

Figures 18a and 18b represent the response diagrams of the Te-2 and 10st-PTED frames providing the highest PUF. Finally, the mean response diagrams of Te-2, 10st- PTED, and 10st-MRF are displayed in Figure 18c for better comparison, which demonstrtaes a decrease in the response values of the maximum and residual drift, RMSAcc, and MaxAcc in Te-2 and 10st-PTED frames relative to that of frame with conventional welded connections in all Floors.

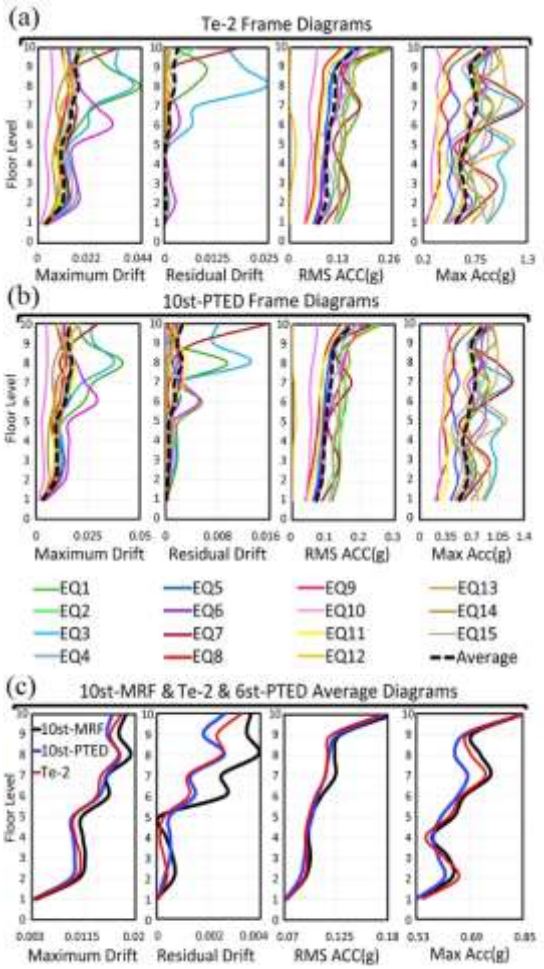

Figure 18. Schematic Diagrams of Te-2 (a), 10st-PTED (b) and average of Te-2, 10st-PTED and 10st-MRF (c) responses

6. CONCLUSION

The present study sought to evaluate the efficiency of the multi-stage improvement's new aproach of moment frames with conventional welded connections using reversible system. In this regard, 6, 10, and 14 post-tensioning states in the 3-, 6-, and 10-story frame were respectively selected in order to assess the feasibility of the suggestion. Additionally, RPI, PUF, and PEF coefficients were applied to examine the intended frames in different states. It should be noted that the PUF coefficient is presented and used for the first time in this paper. Based on the results, the use of PT connections in the lower floors of the frames under study, as the first stage of retrofitting, is a good suggestion.

Among the three-story frames, 3st-PTED frame with a 23.3% performance improvement compared to the MRF one was determined as the most suitable state for attaining the final purpose of upgrading.

Further, the t-1 frame using PT connections in only one floor led to a 15.3% improvement in frame performance (65.9% of the final frame upgrade), and was selected as an option proposed for the first stage of improvement among three-story frames.

Regarding the six-story frames, the s-9 frame using PT connections in the first four floors resulted in enahncing performance by 30.1% compared to that of 6st-MRF, which was even higher than the performance upgrade in the 6st-PTED.

Accordingly, the s-9 frame was selected as the final improvement plan in the study, which represents that finding the situations which can provide the highest performance upgrade without retrofitting all floors is possible if the location of PT connectionts is evaluated in different floors. Furthermore, the performance of s-1 frame enhanced by 11.4% by using PT connections in two floors (37.8% of the final frame upgrade) and was adopted as an option suggested for the first stage of improvement among 6-story frames.

Based on the results of assessing the ten-story frames, the 10-PTED frame was obtained as the most suitable state for achieving the final goal of improvement. In addition, it increased performance by 14.2% compared to that of 10st-MRF frame. Further, the Te-2 frame using PT connections in four floors enhanced performance as 8.5% (60.1% of the final frame upgrade) and was selected as an option proposed for the first stage of improvement among the ten-story frames.

Finally, upgrading frame performance using PT connections during multi-stagecan lead to a good performance in each stage, along with economic savings.

7. REFERENCES

1. Cheok, G.S. and Lew, H.S. "Performance of Precast Concrete Beam-to-column Connections Subject to Cyclic Loading." ***PCI Journal,*** Vol. 36, No. 3, (1991), 56-67. DOI: 10.15554/pcij.05011991.56.67
2. Priestley, M.N. and Tao, J.R. "Seismic Response of Precast Prestressed Concrete Frames with Partially Debonded Tendons." ***PCI Journal,*** Vol. 38, No. 1, (1993), 58-69. DOI: 10.15554/pcij.01011993.58.69
3. Kurama, Y., Pessiki, S., Sause, R. and Lu, L.W. "Seismic Behavior and Design of Unbonded Post-tensioned Precast Concrete Walls." ***PCI Journal,*** Vol. 44, No. 3, (1999), 72-89. DOI: 10.15554/pcij.05011999.72.89
4. Ricles, J.M., Sause, R., Garlock, M.M. and Zhao, C. "Posttensioned Seismic-resistant Connections for Steel Frames." ***Journal of Structural Engineering,*** Vol. 127, No. 2, (2001), 113-121. DOI: 10.1061/(ASCE)0733-9445(2001)127:2(113)
5. Ricles, J.M., Sause, R., Peng, S.W. and Lu, L.W. "Experimental Evaluation of Earthquake Resistant Posttensioned Steel Connections." ***Journal of Structural Engineering,*** Vol. 128, No. 7, (2002), 850-859. DOI: 10.1061/(ASCE)0733-9445(2002)128:7(850)
6. Garlock, M.M., Ricles, J.M. and Sause, R. "Experimental Studies of Full-scale Posttensioned Steel Connections." ***Journal of Structural Engineering,*** Vol. 131, No. 3, (2005), 438-448. DOI: 10.1061/(ASCE)0733-9445(2005)131:3(438)
7. Gerami, M. and Khatami, M. "The Effects of Initial Post Tensioning Force on Seismic Behavior of Steel Moment Resisting Frames by Post-tensioned Connections." ***Sharif Journal of Civil Engineering,*** Vol. 33, No. 1, (2017), 107-115(In Persian). DOI: 10.24200/j30.2017.1101
8. Azizi, M. and Siahpolo, N. "Evaluating the Effect of Strength and Geometry Parameters of Angle on Behavior of Post-Tensioned Steel Connection with Top and Bottom Angles." ***Journal of Structural and Cunstruction Engineering,*** Vol. 24, No. 2, (2019), 193-210, DOI: 10.22065/JSCE.2018.97060.1311
9. Saberi, V., Gerami, M. and Kheyroddin, A. "Seismic rehabilitation of bolted end plate connections using post-tensioned tendons" ***Engineering Structures,*** Vol. 129, (2016), 18-30. DOI: 10.1016/j.engstruct.2016.08.037
10. Akhavan Salmassi, M., Gerami, M. and Heidari Tafreshi, A. "Evaluation of Flexible Steel Frame Structures with Post Tensioned Cables to Sequences Far From Fault." ***Journal of Structural and Construction Engineering,*** Vol. 6, Special Issue 3, (2019), 221-234, DOI: 10.22065/JSCE.2018.101782.1350
11. Christopoulos, C., Filiatrault, A., Uang, C.M. and Folz, B. "Posttensioned Energy Dissipating Connections for Moment-resisting Steel Frames." ***Journal of Structural Engineering,*** Vol. 128, No. 9, (2002), 1111-1120. DOI: 10.1061/(ASCE)0733-9445(2002)128:9(1111)
12. Wang, D.Numerical and experimental studies of self-centering post-tensioned steel frames. State University of New York at Buffalo, 2007.
13. Chancellor, N.B., Eatherton, M.R., Roke, D.A. and Akbaş, T. "Self-centering Seismic Lateral Force Resisting Systems: High Performance Structures for the City of Tomorrow." ***Buildings,*** Vol. 4, No. 3, (2014), 520-548. DOI: 10.3390/buildings4030520
14. Kim, H.J. and Christopoulos, C. "Friction Damped Posttensioned Self-centering Steel Moment-resisting Frames." ***Journal of Structural Engineering,*** Vol. 134, No. 11, (2008), 1768-1779. DOI: 10.1061/(ASCE)0733-9445(2008)134:11(1768)
15. Naghipour, M. Nemati, M. Doostdar, HM. "Experimental Study and Modeling of Reinforced Concrete Beams Strengthened by Post-Tensioned External Reinforcing Bars." ***International Journal of Engineering, Transactions A: Basics,*** Vol. 23, No. 2, (2010), 127-144.
16. Sarvestani, H.A. "Cyclic Behavior of Hexagonal Castellated Beams in Steel Moment-resisting Frames with Post-tensioned Connections." ***Journal of Structures,*** Vol. 11, (2017), 121-134. DOI: 10.1016/j.istruc.2017.05.001
17. Zhao, Z., Jian, X., Liang, B. and Liu, H. "Progressive Collapse Assessment of Friction Damped Post-tensioned Steel Frames Based on a Simplified Model." ***Journal of Structures,*** Vol. 23, (2020), 447-458. DOI: 10.1016/j.istruc.2019.09.005
18. Al Kajbaf, A., Fanaie, N. and Najarkolaie, K.F. "Numerical Simulation of Failure in Steel Posttensioned Connections Under Cyclic Loading." ***Engineering Failure Analysis,*** Vol. 91, (2018), 35-57. DOI: 10.1016/j.engfailanal.2018.04.024
19. Nateghi, F. Vatandoost, A."Seismic Retrofitting RC Structures With Precast Prestressed Concrete Braces-ABAQUS FEA Modeling." ***International Journal of Engineering, Transactions C: Aspects,*** Vol. 31, No. 3, (2018), 394-404. DOI:10.5829/ije.2018.31.03c.01
20. Sharbati, R., Hayati, Y. and Hadianfard, M.A. "Numerical Investigation on the Cyclic Behavior of Post-tensioned Steel Moment Connections with Bolted Angles." ***International Journal of Steel Structures,*** Vol. 19, No. 6, (2019), 1840-1853. DOI: 10.1007/s13296-019-00247-x
21. Guan, X., Burton, H. and Moradi, S. "Seismic Performance of a Self-centering Steel Moment Frame Building: From Component-level Modeling to Economic Loss Assessment." ***Journal of Constructional Steel Research,*** Vol. 150, (2018), 129-140. DOI: 10.1016/j.jcsr.2018.07.026
22. CSI PERFORM-3D.Nonlinear Analysis and Performance Assessment for 3D Structures, Version4. Computers and Structures, Inc., Berkeley, California, 2006.
23. Shen, J. and Akbaş, B. "Seismic Energy Demand in Steel Moment Frames." ***Journal of Earthquake Engineering,*** Vol. 3, No. 04, (1999), 519-559. DOI: 10.1080/13632469909350358
24. Apostolakis, G. Evolutionary aseismic design of self-centering post-tensioned energy dissipating steel frames. State University of New York at Buffalo, 2006.
25. Apostolakis, G., Dargush, G.F. and Filiatrault, A. "Computational Framework for Automated Seismic Design of Steel Frames With Self-centering Connections." ***Journal of Computing in Civil Engineering,*** Vol. 28, No. 2, (2014), 170-181. DOI: 10.1061/(ASCE)CP.1943-5487.0000226
26. Applied Technology Council, Quantification of building seismic performance factors. US Department of Homeland Security, FEMA, 2009.
27. Tafreshi, A.M.H. and Gerami, M. "Implementing posttensioned connections only in some floors of steel moment frames." ***Journal of Structures,*** Vol. 31, (2021), 98-110. DOI: 10.1016/j.istruc.2021.01.080
28. Qiu, C., Zhao, X., & Zhu, S. "Seismic upgrading of multistory steel moment-resisting frames by installing shape memory alloy braces: Design method and performance evaluation." ***Structural Control and Health Monitoring,*** Vol. 27, No. 9, (2020), e2596. DOI: 10.1002/stc.2596

Persian Abstract

چکیده

در سال‌های اخیر مطالعات گسترده‌ای در زمینهٔ سیستم‌های خودمرکزگرای فولادی توسّط محققین صورت پذیرفته که بسیاری از ابهامات در زمینه استفاده از چنین سیستم‌هایی در بهسازی قابهای موجود را برطرف نموده‌است. با توجه به هزینه‌های اجرای کل پروژه بهسازی در یک مرحله و همچنین مواردی نظیر عدم امکان توقف کاربری تمامی طبقات در برخی از ساختمان‌های موجود، روش چند مرحله‌ای بهسازی با استفاده از سیستم‌های خودمرکزگرا در این تحقیق پیشنهاد و بررسی گردیده‌است. در این راستا در مرحله اول با صرف بودجه و زمان اجرای بهسازی کمتر، اقدام به بهسازی بخشی از طبقات صورت می‌پذیرد و در ادامه، مرحله بعدی بهسازی اجرا میگردد. بر این اساس با اجرای مرحله اول بهسازی عملکرد قاب تا حدود مناسبی ارتقا پیدا میکند و همچنین اقدامات صورت پذیرفته در مرحله اولیه بخشی از طرح نهایی بهسازی می‌باشد. در این تحقیق ضرایب PUF و PEF به منظور انتخاب مناسب ترین الگوی بکارگیری اتصالات پس‌کشیده در طبقات مختلف، معرّفی و مورداستفاده قرارگرفته‌شده‌است. پس از انجام تحلیل‌های‌تاریخچه زمانی بر قاب‌های سه، شش و ده طبقه، الگویی برای بهسازی چند مرحله‌ای هر قاب با انتخاب الگوی مناسب استفاده از اتصالات پس‌کشیده در طبقات، پیشنهاد گردیده بنحویکه در مرحله اول طرح پیشنهادی در قاب سه طبقه ۱۵/۳ درصد، قاب شش طبقه ۱۱/۴ درصد و قاب ده طبقه ۸/۵ درصد ارتقای عملکردی ایجاد گردیده است.